Article

Not peer-reviewed version

Consumption of Limosilactobacillus fermentum Inhibits Corneal Damage and Inflammation in Dry Eye Disease Mice Model through Regulating the Gut Microbiome

Kippeum Lee , Hyeonjun Gwon , Jae Jung Shim , Joo Yun Kim * , Jae Hwan Lee

Posted Date: 21 February 2024

doi: 10.20944/preprints202402.1226.v1

Keywords: Corneal disease; Dry eye; Limosilactobacillus fermentum; Gut-eye axis microbiome; pro-inflammatory regulation; Tight junction

Article

Consumption of *Limosilactobacillus fermentum* Inhibits Corneal Damage and Inflammation in Dry Eye Disease Mice Model through Regulating the Gut Microbiome

Kippeum Lee †, Hyeonjun Gwon, Jae Jung Shim, Joo Yun Kim * and Jae Hwan Lee

[1] R&BD Center, hy Co Ltd., 22, Giheungdanji-ro 24 beon-gil, Giheung-gu, Gyeonggi-do 17086, Korea; joy4917@hanmail.net (K.L.); hjgwon@hy.co.kr (H. K.); jjshim@hy.co.kr (J.J.S.); monera@hy.co.kr (J.Y.K); jaehwan@hy.co.kr (J.W.L)

* Correspondence: monera@hy.co.kr (J.Y.K)

† First author.

Abstract: (1) The present study investigated the effect of orally administered *Limosilactobacillus fermentum* HY7302 (HY7302) on the relationship between ocular tissue and the microbiome in the corneal injured dry eye mice model. (2) 0.1% benzalkonium chloride (BAC) was applied to the ocular surface for 14 days to induce corneal injury in male Balb/c mice. During the BAC treatment period, HY7302 (1×10^8 CFU/kg/day or 1×10^9 CFU/kg/day) or omega-3 positive control (200 mg/kg/day) were administered orally (n = 8/group). To examine signaling pathways affected by HY7302 treatment, the *in vitro* effects of HY7302 on tight junctions and the inflammatory response were investigated in a mouse colon epithelial cell line, CMT-93. (3) BAC exposure decreased tear production, induced ocular inflammation and corneal epithelial detachment, and altered gut microbiota. However, oral administration of HY7302 restored tear secretion and decreased corneal epithelial detachment in BAC-treated corneal injury mice. Further, HY7302 alleviated corneal inflammation via modulation of matrix metalloproteinase-9 (MMP-9) expression and alterations in gut microbiota composition. (4) These findings suggest that the gut–eye axis interaction between gut microbiota and eye tissue affects disease severity in corneal injury, and that alteration of the microbiota by HY7302 could improve eye health by regulating the inflammatory response.

Keywords: corneal disease; dry eye; *Limosilactobacillus fermentum*; gut-eye axis microbiome; pro-inflammatory regulation; tight junction

1. Introduction

Dry eye (DE), is a multifactorial disease of the ocular surface caused by impairment of tear production and cornea damage, which affects 5–40% of adults over 40 years of age [1]. The prevalence of DE is steadily increasing, and DE is one of three major eye diseases rapidly increasing in the elderly [2]. The primary symptoms of DE are stiffness, vision blurring, eye fatigue, and eye congestion. Dysfunction of tear film can cause damage to the cornea and other epithelial eye tissue, preventing them from functioning correctly [3]. Also, DE is closely related to inflammation-induced tear film instability and ocular surface [4]. Because DE can result epithelial lesions or local inflammation reaction, leading to a deterioration of ocular surface defense mechanisms, dysfunction, and cellular degeneration of conjunctiva and cornea apart [5]. Therefore, it is meaningful to find attempts to therapeutic approach to DE treatments. One of approaches, artificial tears containing hyaluronic acid or cyclosporine A are used to treat DE, but provide only temporary symptomatic relief [6]. Long-term application of these agents can have adverse effects such as an corneal and ocular hypertension, infection, and inflammation [7]. Benzalkonium chloride (BAC) is the most commonly used preservative in topical artificial tears products. Although BAC have amphiphilic, high water-soluble characters, and antimicrobial effect, long-term use can occur side effect including DE and ocular

 doi:10.20944/preprints202402.1226.v1

inflammation [8,9]. Even recent studies reported that BAC can reach the posterior eye and optic nerve [10,11].

Cornea injury is a representative feature of dry eyes, is characterized by ocular surface inflammation and destruction of the tear film due to up-regulation of inflammatory cytokines [12]. Also, ocular inflammation is considered the hallmarks of DE. Production of pro-inflammatory triggers, including interleukin-20 (IL-20) and tumor necrosis factor-α onto the ocular epithelial surface and subsequent damage causes tear film dysfunction and ultimately DE [13]. Metalloproteinases (MMPs) are positively associated with the severity of inflammation in the conjunctiva tissue, and recent studies have identified MMPs as a potential therapeutic target for DE [14]. MMPs also disrupt tight junctions essential for maintenance of the corneal barrier. In DE, matrix metalloproteinase-9 (MMP-9) levels are increased in the tears and ocular epithelial surface [15]. Exposure of the cornea to desiccating stress increases corneal epithelial permeability, which is regulated in part by increased MMP-9 level [16-18]. Also, the pro-inflammatory cytokine IL-20 is involved in the pathogenesis of inflammatory DE disease. A recent study identified that circulating level is significantly increased in DE patient tears and corneas, and in induced DE models [19].

The gut microbiota regulates host physiological processes via strengthening gut tight junctions and regulating the intestinal epithelium, with improved function associated with increased microbial diversity [20]. The composition and activity of the gut microbiota affect host health by causing changes in metabolic activity or changes in local distribution [21]. For instance, certain symbiotic bacteria such as Bifidobacterium can prevent colonization of pathogenic bacteria by reducing the intestinal pH [22]. Also, with recent enhanced understanding of the important role of gut microbiome, the host inflammation response and the pathogenesis of ocular disease also has been brought to attention [23]. Recent studies have reported an association between ocular disease and the microbiota profile of the host intestine. This is called the 'gut-eye axis', which indicates that changes in the gut microbiome alter host immunity, with consequential influence for ocular health and disease [24,25]. Furthermore, the gut microbiome is associated with myriad pathophysiological processes in the host, especially chronic inflammatory diseases [26-29]. Therefore, probiotics have recently attracted attention as a potential dietary supplement to prevent inflammation. One of the major mechanisms of immune system-related benefits of probiotics studied *in vitro* and *in vivo* studies is to enhance the epithelial barrier and regulate inflammatory cytokine production. Indeed, numerous studies have reported that *Lactobacillus* and *Bifidobacterium* have the ability to accelerate the anti-inflammatory process and reduce the production of the pro-inflammatory cytokines IL-1b or IL-6.

Bacteria of the phylum Firmicutes are some of the most important probiotic bacteria of the gut microbiome. Firmicutes are widely distributed in nature, and include *Limosilactobacillus fermetum*, *Limosilactobacillus ruuteri, Lactobacillus acidophilus*, *Lacticaseibacillus casei*, and *Lactobacillus delbrueckii subsp. Bulgaricus.* Especially, *Limosilactobacillus fermentum* (*L. fermentum*) is an obligately heterofermentative microbiota that ferments carbohydrates to produce lactic acid, ethanol, acetic acid, and carbon dioxide [30]. Recent studies have reported beneficial effects of *L. fermentum* in obesity, cardiovascular disease, metabolic mellitus, and gastrointestinal barrier dysfunction [31-34]. It is also known through animal experiments that *L. fermentum* acts as an antimicrobial and antioxidant modulator [35]. In our previous study, we identified that oral administration of *Limosilactobacillus fermentum* HY7302 (HY7302) improves DE symptoms in the mice model [36]. However, the molecular mechanisms of the effects of probiotic intake on ocular tissues have not yet been elucidated. Therefore, in this study, to understand the efficacy and molecular mechanisms of probiotics on DE-induced corneal damage, we determined the signaling regulation of inflammatory and apoptotic factors in ocular tissues after HY7302 intake in BAC-induced DE mice. To understand the mechanisms for the therapeutic effects of HY7302 in DE, it is essential to delineate the role of the gut–eye axis and microbiome in regulating DE pathology. Thus, we investigated the correlation effect of HY7302 probiotics with the intestinal microbiome of corneal damaged mice in this study.

 doi:10.20944/preprints202402.1226.v1

2. Materials and Methods

2.1. Animal Study

Six-week-old male Balb/c mice (ORIENT, Seongnam-si, Republic of Korea) were used in the study. All in vivo studies were approved by the Institutional Animal Care and Use Committee (IACUC number P235002) of NDIC Co., Ltd in Korea and adhered to the guidelines of code of practice for the housing and care of Animals used in scientific procedures. Prior to experiments, mice were acclimatized for 1 week with ad libitum access to water and food on a 12 h light/12 h dark cycle. Room temperature was 23 ± 2°C and relative humidity was 40–70%. Mice were randomly allocated to one of five groups: CON, non-DE control group; DE, topical 0.1% BAC; DE + Omega3, topical 0.1% BAC + oral Omega3 (200 mg/kg/day); DE + HY7302L, topical 0.1% BAC + oral HY7302 (108 CFU /kg/day); DE + HY7302H, topical 0.1% BAC + oral HY7302 (109 CFU/kg/day). (n = 8 mice/group). To induce DE, mouse eyes were exposed to 0.1% BAC (Sigma-Aldrich, St. Louis, MI, USA) dissolved in phosphate buffered saline, with 5 μL/eye applied twice daily to the ocular surface for 14 days. During the same period, HY7302 (1×10^8 CFU/kg/day or 1×10^9 CFU/kg/day) dissolved in 0.5% aqueous carboxymethylcellulose solution were administered orally. Omega-3 fatty acids in 0.5% aqueous carboxymethylcellulose solution was orally gavaged (200 mg/kg/day) in a positive control group.

2.2. Blood parameter analysis

Blood was collected via the abcominal vein immediately after euthanasia, and serum was prepared by centrifuging at 3,000 RPM for 20 min. Serum concentrations of MMP-9 (ab253227) and IL-20 (ab235645) were measured using commercial assay kits (Abcam, Cambridge, UK).

2.3. Measurement of tear volume, corneal fluorescein score, and tear break-up time

Tear volume was measured in each mouse following abdominal injection of 10 mg/kg xylazine/100 mg/kg ketamine. Tear amounts were measured using Schirmer's test strips (Bio Color Tear Test, Bio Optics, Seongnam-si, Republic of Korea). Tear break-up time (TBUT) was determined using a cobalt blue slit lamp after corneas were treated with 0.5% fluorescein solution on day 14 of BAC treatment. The time (sec) until appearance of the first crack line on the dryed tear film layer was recorded. Subsequently, corneas were washed with a troterin antidote treatment (Alcon, Seoul, Republic of Korea). Flouorescein sodium solution (0.1%) was appied to the cornea, and corneal images were captured under blue light (Micron-IV, Phoenix, Kawasaki, Japan). The corneal fluorescein staining (CFS) score was caculated using a 0–3 point scale. The cornea was divided into into five areas, which were scored individually, and the values were added to obtain the combined score.

2.4. Histological analysis

Eyes were fixed with 4% paraformaldehyde and embedded in paraffin. Sections were obtained, stained with hematoxylin and eosin (H&E), and analyzed by light microscopy (Nikon Eclipse E600 microscope, Nikon Corporation, Tokyo, Japan). The number of corneal epithelium detachments per area was calculated using Image J software.

2.5. Western blotting

Mice eye tissues or cells were lysed using pro-prep buffer (iNtRON Biotechnology Inc., Seoul, Korea) containing proteinase and phosphatase inhibitors. Homogenates were centrifuged at 10,000 × g for 15 min at 4°C and supernatants were collected. Total protein concentration was measured using a Bio-Rad protein assay kit (Bio-Rad, Hercules, CA, USA). Protein lysates (18 μg) were seperated on 4–15% Precast gradient SDS-PAGE gels and transferred to PVDF membranes. Membranes were incubated at 4°C overnight with primary antibodies in Tris-buffered saline containing 0.05% Tween-20 (TBS-T) and 5% skimmilk. After washing with TBS-T, membranes were incubated in 5% non-fat dried milk containing secondary antibody conjugated to IgG horseradish peroxidase for 1 h. Protein

 doi:10.20944/preprints202402.1226.v1

bands were visualized using EZ-Western Lumi Femto (DoGenBio, Seoul, Korea) and an LAS-4000 imager (GE Healthcare Life Sciences, Marlborough, MA, USA), which was also used to quantify band density. B-cell lymphoma 2 (Bcl-2 D17C4, cs3498), Bcl-2-associated X protein (BAX, cs2772), Cleaved Caspase-3 (Cleaved Cas-3 Asp175, 5A1E, cs9664), Glyceraldehyde 3-phosphate dehydrogenase (GAPDH 14C10, cs2118), phospho-p44/42 MAPK (p-ERK Erk1/2 137F5, cs4695), p44/42 MAPK (ERK Erk1/2 Thr202/Tyr204, cs4370), phospho-c-Jun N-terminal kinases (p-JNK Thr183/Tyr185 81E11, cs4668), c-Jun N-terminal kinases (JNK, cs9252), Interleukin 1 beta (IL-1β D3H1Z, cs12507), Matrix Metalloproteinase-9 (MMP-9 E7N3Y, cs24317), and Anti-rabbit IgG HRP-linked secondary antibodies were purchased from Cell signaling (Cell Signaling Technology, Massachusetts, USA).

2.6. Microbiome 16s rRNA gene amplification and sequencing

Sequencing libraries with amplified V3-V4 regions were generated according to the Illumina 16s Metagenomic Sequencing Library Preparation Guide (Illumina, San Diego, CA, USA). Input gDNA (2 ng) was PCR-amplified with 5× reaction buffer, 1 mM dNTP mix, 500 nM of each universal F/R PCR primer, and Herculase II fusion DNA polymerase (Agilent Technologies, Santa Clara, CA, USA). Thermal cycling for the first PCR step included 3 mins denaturation at 95°C, 25 cycles of 30 s at 55°C and 30 s at 72°C, followed by a 5 min final extension at 72°C. For sequencing, the V3-V4 regions of the bacterial 16S rRNA gene were amplified using primer set 341F (5′-TCGTC GGCAGCGTCAGATGTGTATAAGAGACAGCCTACGGGNGGCWGCAG-3′) and 806R (5′-GTCTCGTGGGCTCGGAGATGTGTATAAGAGACAGGACTACHVGGGTATCTAATCC-3′). PCR products were purified using AMPure beads (Agencourt Bioscience, Beverly, MA, USA). Following purification, 2 μL PCR product from the first step was PCR-amplified for final library construction using NexteraXT Indexed Primer (Illumina, San Diego, CA, USA). Thermal cycling of the second PCR step was performed as described for the first step with 10 cycles. qPCR was conducted according to the qPCR Quantification Protocol Guide (KAPA Library Quantification kits for Illumina Sequencing platforms) and quantified using a TapeStation D1000 ScreenTape (Agilent Technologies, Waldbronn, Germany). All datasets have been deposited in NCBI Gene Expression Omnibus under accession number PRJNA1065618.

2.7. Microbiome Bioinformatic Analysis of 16s rRNA Sequencing Data

The 16s rRNA amplicon sequence data were analyzed using the QIIME2 platform (version 2023.9) [37]. Sequences were demultiplexed using the q2-demux plugin and sequences with low quality scores were removed using the DADA2 plugin, generating an amplicon sequence variants (ASVs) table [38]. ASVs were aligned using the MAFFT plugin, and were used to generate a rooted phylogenetic tree for phylogenetic diversity analysis using FastTree 2 [39,40]. Taxonomy analysis was performed using the QIIME2 feature classifier plugin, with a 99% identity threshold to the Silva 138 database [41,42]. Alpha diversity metrics of observed features were calculated to measure microbial diversity. A non-parametric Kruskal-Wallis test was used to determine the statistical significances of differences in microbial diversity. Unweighted UniFrac distance metrics were analyzed using Principle Coordinate Analysis (PCoA) [43,44], and the statistical significance of differences in PCoA plots between groups was assessed using permutational multivariate analysis of variance (PERMANOVA). Furthermore, using the Linear discriminant analysis effect size (LEfSe) method, significant differences in the relative abundance of bacterial composition between the HY7302 Low and High groups and DE groups were identified (LDA > 3.0). Correlations between gut microbiota and DE parameters (MMP9 IL-20, TV, TBUT, and Detachment)were calculated by using the Spearman's rank correlation coefficient in the R software package.

2.8. Cell culture

The mouse CMT-93 (CCL-223) colon epithelial cell line was purchased from ATCC (Manassas, VA, USA). CMT-93 cells were cultured in DMEM/F12 containing 10% FBS and 1% penicillin/streptomycin (P/S) in a humidified 5% CO_2 incubator at 37°C. HY7302 probiotics were

 doi:10.20944/preprints202402.1226.v1

prepared as a 1 × 10^{10} CFU/mL stock solution in distilled water and then diluted in medium to final concentrations of 1 × 10^{6} CFU/mL or 1 × 10^{7} CFU/mL. Cells were treated with 100 ng/mL TNFα to increase epithelial tight junction permeability.2.9. RNA isolation and quantitative polymerase chain reaction (q-PCR) analysis

2.9. RNA isolation and quantitative polymerase chain reaction (q-PCR) analysis

RNA was extracted using Trizol and 2 μg total RNA was reverse-transcribed to cDNA using a commercial kit (Maxime RT PreMix Kit, Intronm Seongnam, Korea). cDNA was analyzed by qPCR (Applied Biosystems, Carlsbad, CA, USA) using the TaqMan Probe-Based Gene Expression analysis system in combination with the TaqMan Gene Expression Master Mix (Applied Biosystems, Waltham, MA, USA). Tight juction protein-1 (TJP-1, Mm01320638_m1), tight juction protein-2 (TJP-2, Hs00910543_m1), Ocludin (Mm00500910_m1), Claudin-4 (CLDN-4, Mm00515514_s1), tumor necrosis factor (TNF, Mm00443258_m1), MMP-9 (Mm00442991_m1), and Interleukin-6 (IL-6, Mm00446190_m1) transcripts were quantified using gene-specific primers. Target gene mRNA levels were normalized against the corresponding level of GAPDH mRNA (Mm99999915_g1). To compare gene expression levels between groups, relative mRNA levels were calculated using the $2^{(-\Delta\Delta CT)}$ method.

2.10. Statistical analyses

mRNA and protein data are expressed as means ± standard deviations (SD). Data were analyzed and compared statistically with an unpaired two-tailed Student's t-test using SPSS version 26.0 (IBM, Somers, NY, USA).

3. Results

3.1. HY7302 ameriolated BAC-induced DE symptoms

To examine the differences in physiological characteristics between control and DE mice, the eyes of mice in the DE groups were exposed to benzalkonium chloride (BAC) twice daily for 14 days. During the same period, mice received once daily oral administration of vehicle control, low-concentration HY7302 (1 × 10^{8} CFU/kg/day), high-concentration HY7302 (1 × 10^{9} CFU/kg/day), or Omega3 (200 mg/kg/day) as a positive control. To evaluate corneal epitheliopathy following oral administration of HY7302, corneal fluorescein staining was conducted, with representative images shown in Figure 1A. Significant differences in CFS scores were present between non-DE control (CON) and DE groups. CFS scores in HY7302 groups were similar to that of the omega-3 group, with all experimental groups significantly decreased compared with the DE group (Figure 1B). Furthermore, BAC treatment significantly decreased TBUT by 36% and tear volume (TV) by 66% relative to CON. Treatment with 1 × 10^{8} CFU/kg/day HY7302 recovered TBUT to 128% and TV to 223% relative to the vehicle-treated DE group. Treatment with 1 × 10^{9} CFU/kg/day HY7302 increased TBUT to 137% and TV to 238% relative to the vehicle-treated DE group (Figure 1C-D). Positive control, omega3-treated group showed increased TBUT to 130% and TV to 228% relative to the DE group.

 doi:10.20944/preprints202402.1226.v1

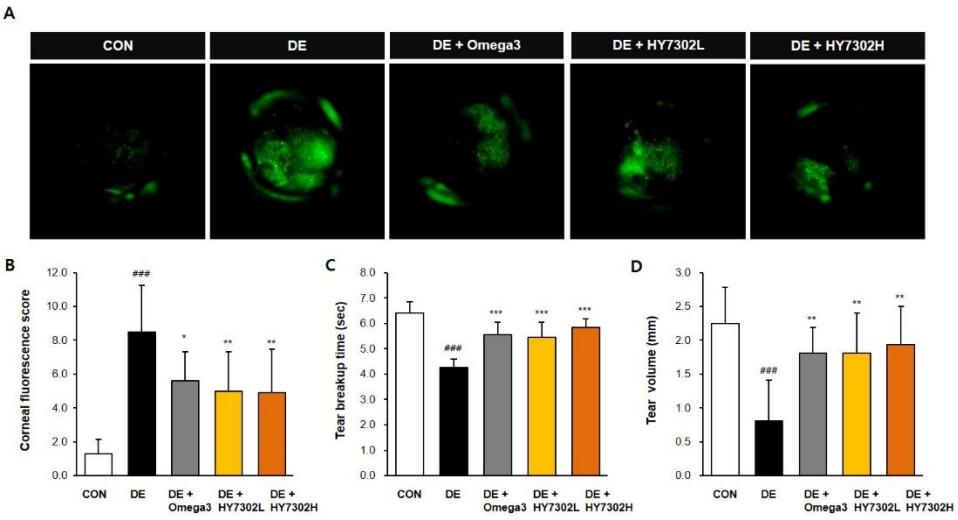

Figure 1. Effect of HY7302 on corneal fluorescein score, tear break-up time, and tear volume. (A-B) Corneal fluorescein images and corneal fluorescein sodium staining (CFS) scores in DE mice. **(C)** Tear break-up time as detected with commercial fluorescein strips. **(D)** Tear volume as measured by Schirmer's test. CON, non-DE control group; DE, topical 0.1% BAC; DE + Omega3, topical 0.1% BAC + oral Omega3 (200 mg/kg/day); DE + HY7302L, topical 0.1 % BAC + oral HY7302 (10^8 CFU/kg/day); DE + HY7302H, topical 0.1% BAC + oral HY7302 (10^9 CFU/kg/day). ### p< 0.001 relative to CON. *p < 0.05, **p < 0.01, and ***p<0.001 relative to DE.

3.2. HY7302 improved corneal epithelial damage in BAC-induced cornea damage mice

Folowing 14 days of topical ocular BAC treatment, detached epithelial flaps and damaged corneal basal cells were present in H&E images. However, the epithelial morphology of HY7302- and omega3-treated DE mice was improved compared with the untreated DE group (Figure 2A). Corenal epithelial tissue dissections were counted in each group, with a 60% decrease of dissections in HY7302L-treated animals and a 57% decrease in HY7302H-treated animals relative to the DE group (Figure 2B). Also, omega3 group showed 57% decrease of dissection score compared the DE group.

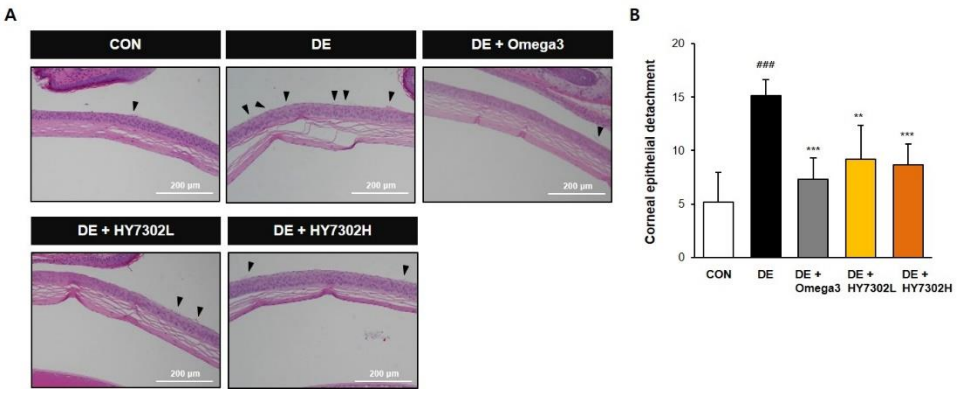

Figure 2. Effect of HY7302 on corneal epithelial detachment. (A) Representative hematoxylin and eosin images of DE mouse corneas. Arrows indicate detaching damaged apical tissue. **(B)** Quantification of corneal epithelial detachment, expressed as means ± SD (N = 4 eyes/group). ###p < 0.001 relative to CON. **p < 0.01 and ***p < 0.001 relative to DE.

3.3. HY7302 regulation of pro-inflammatory factors in BAC-induced cornea damage mice

Pro-inflammatory regulators initiate immue activation by the corneal epithelia, which is a defining characteristic of DE. Recent studies have identified upregulation of MMPs as a pathologic change in DE pateints and animal models [45,46]. We measured pro-inflammatory protein levels in eye tissues and serum to delineate the molecular mechanisms by which HY7302 alleviated DE (Figure

 doi:10.20944/preprints202402.1226.v1

3A-B). p-ERK/ERK ratio, p-JNK/JNK ratio, IL-1β level, and MMP-9 level were significanlty increased in eye tissue of DE mice. HY7302 administration decreased p-ERK/ERK ratio, p-JNK/JNK ratio, and IL-1β level relative to the untreated DE group in a dose-dependent manner. MMP-9 levels were also dereased in HY7302-treated DE mice. By contrast, Omega3 treatment did not affect p-JNK/JNK ratio or IL-1β level, but decreased MMP-9 level. Serum MMP-9 levels were 3.2-fold higher in DE mice than in CON mice (Figure 3 C-D). Serum MMP-9 levels were significantly decreased by 0.48-fold in HY7302L-treated mice and 0.42-fold in HY7302H-treated mice relative to DE mice, which was more effective than decreased by 0.65-fold in Omega3 treated mice. Lastly, serum IL-20 was significantly decreased by 0.84-fold in HY7302H-treaed mice relative to DE mice, which was more effective than Omega3 treatment.

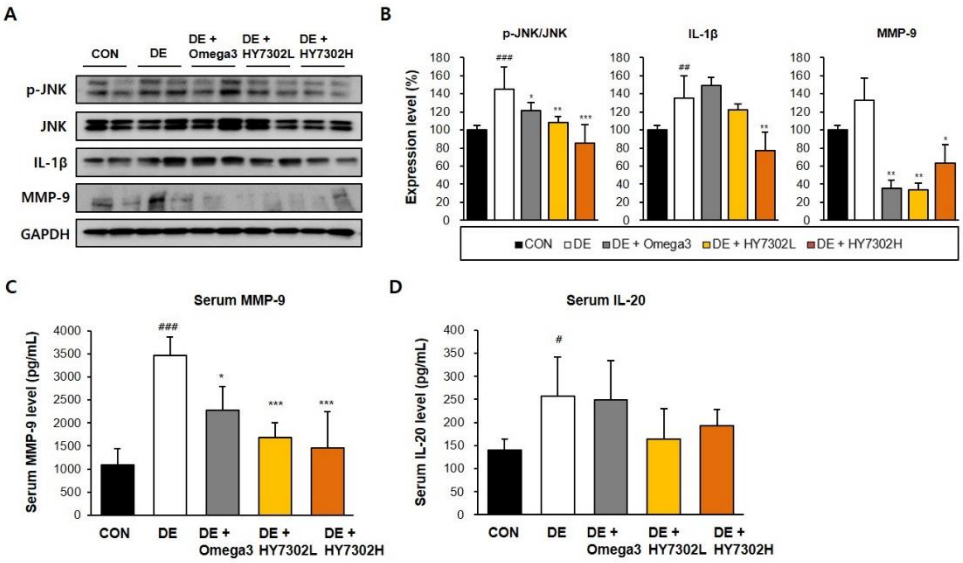

Figure 3. Effect of HY7302 on serum and eye tissue pro-inflammatory factor levels in BAC-induced DE mice. (A) Western blot images of extracellular signal-regulated kinase (ERK), phospho-ERK (p-ERK), c-Jun N-Terminal kinase (JNK), phospho-JNK (p-JNK), matrix metalloproteinase-9 (MMP-9), inteleukin-1 beta (IL-1β), and glyceraldehyde 3-phosphate dehydrogenase (GAPDH). **(B)** quantification of phosphoprotein ratios or protein levels relative to CON. Serum concentrations of **(C)** matrix metalloproteinase-9 (MMP-9) and **(D)** interleukin-20 (IL-20) were measured by ELISA. #p < 0.05 and ###p < 0.001 relative to CON. *p< 0.05, **p < 0.01, and ***p < 0.001 relative to DE.

3.4. HY7302 decreased activation of ocular apoptotic pathways in BAC-induced cornea damage mice

To evalutate the effect of HY7302 probiotic treatement on ocular surface apoptosis, protein levels of apoptotic factors were measured by Western blot. BAX and cleaved caspase-3 levels were increased in eye tissue of DE mice relative to CON mice. Bcl-2 levels were significantly decreased in DE mice relative to CON mice. Treatment with HY7302 reversed the effects of DE on blc-2 and cleaved caspase-3 levels in a dose-dependent manner. However, BAX levels were significantly decreased by HY7302L treatment, but non-significantly decreased by HY7302H treatment. Contrastingly, treatment with Omega3, which was used as a positive control, did not affect apoptotic factor levels in DE mice.

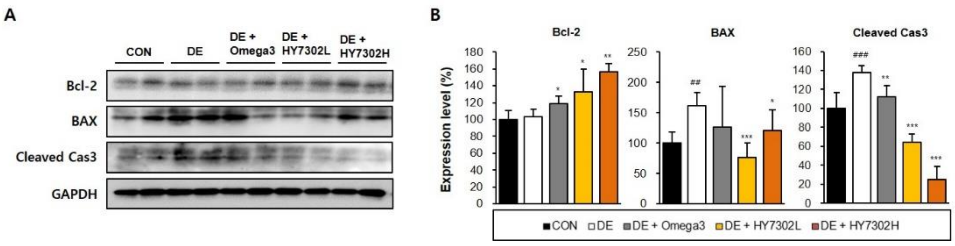

 doi:10.20944/preprints202402.1226.v1

Figure 4. Effect of HY7302 on apoptotic factor levels in eye tissue of BAC-induced DE mice. (A) Western blot images of B-cell lymphoma 2 (Bcl-2), Bcl-2-associated X protein (BAX), cleaved Caspase-3 (cleaved Cas3), and Glyceraldehyde 3-phosphate dehydrogenase (GAPDH), and **(B)** quantification of protein levels relative to CON. Statistical significance was determined using a one-way ANOVA followed by a Duncan's test (n = 4). $^{\#}p < 0.05$ and $^{\#\#\#}p < 0.001$ relative to CON. $^{*}p < 0.05$, $^{**}p < 0.01$, and $^{***}p < 0.001$ relative to DE.

3.5. Effect of HY7302 probiotics on microbial diversity and composition in BAC-induced cornea damage mice

The composition of the gut microbiota was analyzed in each treatment group (Figure 5). The alpha diversity of the fecal microbiome community in treatment groups (CON, DE, DE + Omega3, DE + HY7302L, DE + HY7302H) was characterized using the observed index (Figure 5A). There were no significant differences in microbial community diversity between groups according to alpha diversity. However, index data revealed that microbiome richness was modestly decreased in the DE group relative to the CON group. Beta diversity was analyzed by calculating the unweighted UniFrac distance to examine differences in microbial community composition and structure. Significant differences were detected between CON mice and DE mice, and between DE + Omega3, DE + HY7302L, and DE + HY7302H mice relative to DE mice (Figure 5B). This suggested that HY7302 could regulate the microbial community in BAC-induced DE mice. The Spearman correlation of microbiota taxonomic levels with in vivo experimental DE parameters, including serum MMP-9, serum IL-20, TV, TBUT, and corneal epithelial detachment damage of DE, DE + HY7302L, and DE + HY7302H group was determined (Figure 5C). Relative Bifidobacterium abundance positively correlated with TV ($\varrho = 0.48$), while Colidextribacter abundance negatively correlated with TV ($\varrho = -0.41$). Further, Lachnospiraceae family (Lachnospiraceae A2, Lachnospiraceae NK4A136 group, Roseburia, and Blautia) abundance negatively correlated with TV in HY7302-treated groups. TBUT index positively correlated with abundances of family Muribaculaceae, genus Muribaculum, Oscillibacter, Oscillospirales UCG-010, and Bifidobacterium. In most taxonomic analyses, TBUT index was similar to TV. Corneal epithelial detachment was positively correlated with abuncance of Roseburia and Lachnospiraceae NK4A136, and negatively correlated with abunddances of Osillibacter and Osillospirales UCG-010. Seurm MMP-9 levels positively correlated with abundances of family Lachnospiraceae, Lachnospiraceae A2, Lachnospiraceae NK4A136, Roseburia, and Colidextribacter, while seurm MMP-9 levels negatively correlated with abundances of family Muribaculaceae, Muribaculum, Oscillibacter, Oscillospirales UCG-010, Bifidobacterium, and Lactobacillus. Lastly, relative microbiota abundance was evaluated at the species level. Relative abunances of Clostridium leptum and Bacteroides caccae were decreased in the DE group relative to the CON group. The abundance of B. caccae was significantly increased in the DE + HY7302H group relative to the DE group, and was modestly increased in the DE + HY7302L group relative to the DE group. C. leptum (genus Oscillibacter) abundance was decreased in the DE group relative to the CON group, while C. leptum abundance was increased in the DE + HY7302L and DE + HY7302H groups relative to the DE group. Interestingly, HY7302H treatment significantly altered B.pseudolongum abundance compared with the CON and DE groups, which positively correlated with TV.

 doi:10.20944/preprints202402.1226.v1

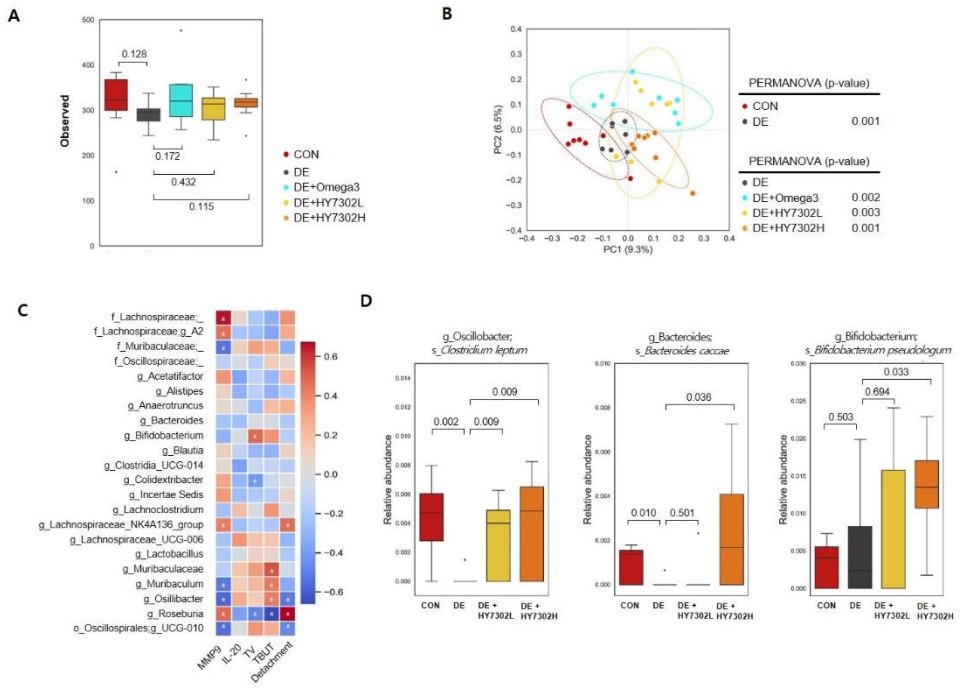

Figure 5. Effect of HY7302 on gut microbiota diversity, Spearman's correlation, and relative species-level abundances in BAC-induced DE mice. (A) Box plots of microbial alpha diversities of each group were calculated using observed features. (B) PCoA plots of the bacterial community using unweighted UniFrac distance and PERMANOVA were used to measure dissimilarity between groups. (C) Spearman's correlation analysis between genus-level taxonomy profiles and DE indicators (serum MMP-9, serum IL-20, TV, TBUT, and corneal epithelial detachment). In the heatmap, red squares indicate positive correlations and blue squares indicate negative correlations. ($^{*}p < 0.05$). (D) Relative changes in abundances of microbiota species (Clostridium leptum, Bacteroides caccae, Bifidobacterium pseudolongum) at baseline and after HY7302 treatment.

3.6. HY7302 increased transcirpt levels of tight junction components and decreased pro-inflammatory factor mRNA levels in the mice CMT93 cell line

CMT93 colon epithelial cells were incubated with different concentrations of HY7302 for 24 h to determine the effect on cell survival. A cell counting kit-8 (CCK8) assay revealed that cell viability was > 90% at all tested HY7302 concentrations, and only the highest concentration, 1×10^9 CFU/mL, had significant toxic effects (Figure 6A). Treatmnet of CMT93 cells with 1×10^6 CFU/mL HY7302 increased mRNA levels of the tight junction components TJP-1 (1.25-fold) and OCLN-1 (1.46-fold), but did not affect CLDN-4 mRNA level (Figure 6B-D). The effect of HY7302 on tight junction integrity in cells challenged with TNFα-induced inflammation (100 ng/mL) was evaluated. In cells stimulated with TNFα (TNF group), mRNA levels of TJP-1 (0.81-fold), OCLN-1 (0.92-fold), and CLDN-4 (0.75-fold) decreased relative to the CON group (Figure 6E-G). mRNA levels of TJP-1 and OCLN-1 were significantly increased in TNFα-stimulated cells treated with HY7302 (TNF + HY7304 group), but CLDN-4 mRNA levels were unchanged (Figure 6E-G). Morever, TNFα stimulation increased the production and release of pro-inflammatory cytokines and MMP-9. mRNA levels of TNF (1.91-fold), MMP-9 (3.41-fold), and IL-6 (6.05-fold) were increased in the TNF group relative to the CON group (Figure 7A-C). Co-treatment with 1×10^6 CFU/mL HY7302 (TNF + HY3702 group) attenuated upregulation of inflammatory factor mRNA levels (TNF 2.48-fold, MMP-9 1.12-fold, and IL-6 5.09-fold relative to CON group, Figure 7 A-C). Similary, TNFα stimulation and HY7302 co-treatment (T + 10^6 and T + 10^7 groups) suppressed p-ERK/ERK ratio, p-p38/p38 ratio, MMP-9 protein level, and IL-1β protein level relative to untreated TNFα-stimulated cells (T group) in a dose-dependent manner (Figure 7D-E).

 doi:10.20944/preprints202402.1226.v1

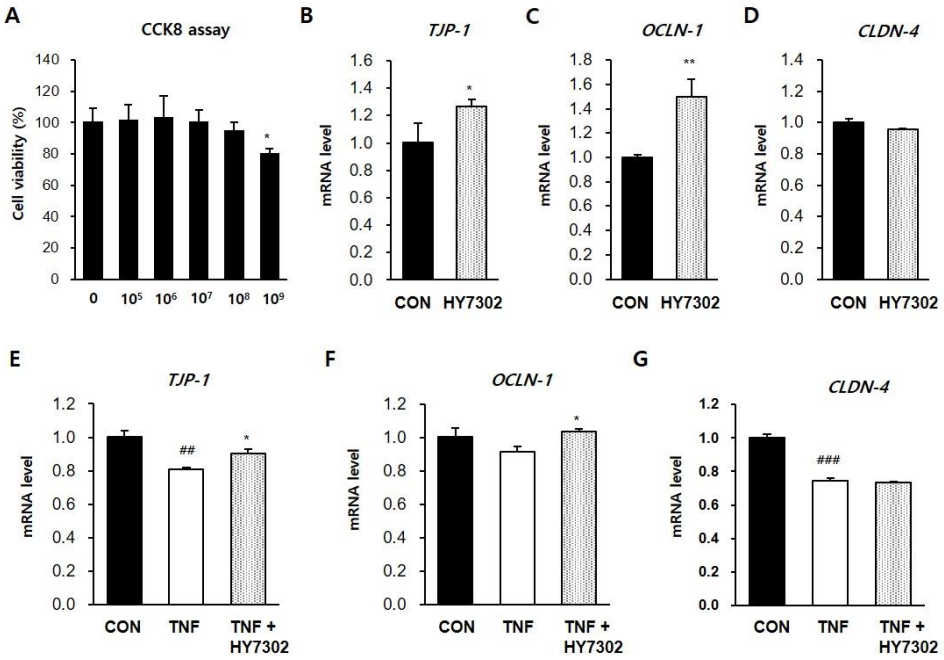

Figure 6. Effect of HY7302 on mRNA levels of tight junction components in TNFα-stimulated CMT93 cells. (A) Cell viability of CMT93 cells following 24 h HY7302 treatment was detected using a Cell Counting Kit-8 (CCK-8) assay. (B-D) mRNA levels of (B) tight junction protein-1 (TJP-1), (C) occuludin-1 (OCLD-1), and (D) Claudin-4 (CLDN-4) in CMT93 cells treated with vehicle (CON group) or 107 CFU/mL HY7302 (HY7302 group) were measured by quantitative-PCR. (E-G) mRNA levels of (E) TJP-1, (F) OCLD-1, and (G) CLDN-4 were measured by qPCR in CMT93 cells treated with vehicle (CON group), 100 ng/mL TNFα (TNF group) or 100 ng/mL TNFα + 107 CFU/mL HY7302 (TNF + HY3702 group). ##p < 0.01 and ###p < 0.001 relative to CON group. *p < 0.05 and **p < 0.01 relative to TNF treated group.

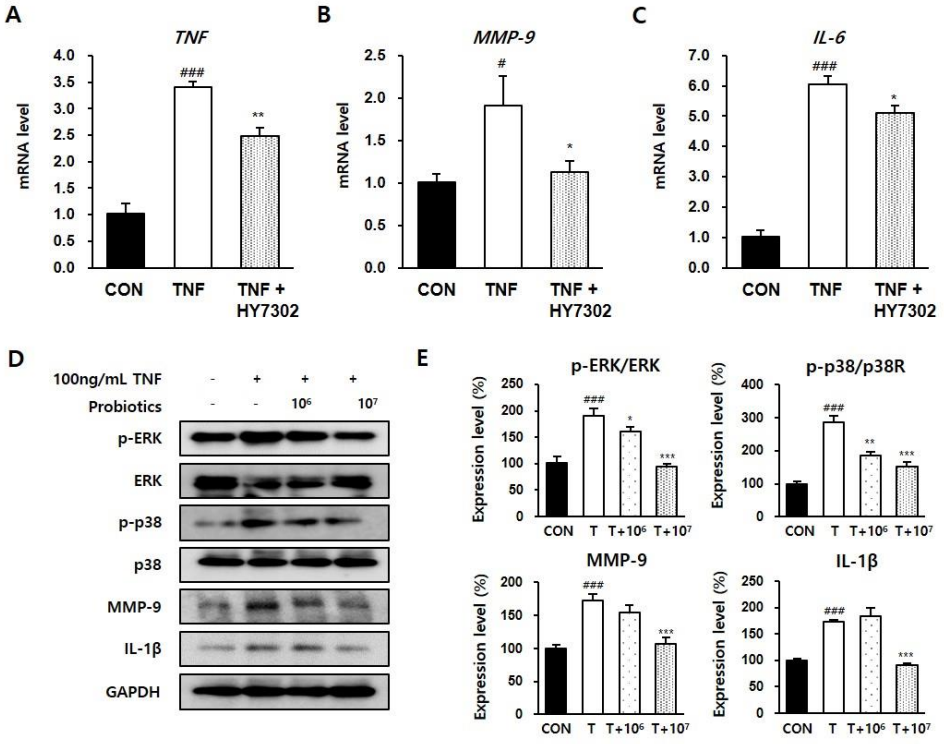

Figure 7. Effect of HY7302 on pro-inflammatory factors in TNFα-stimulated CMT93 cells. (A-C) mRNA levels of (A) tumor necrosis factor *(TNF)*, (B) matrix metalloproteinase-9 *(MMP-9)*, and (C)

 doi:10.20944/preprints202402.1226.v1

inteleukin-6 (IL-6) were measured by qPCR in CMT93 treated with vehicle (CON group), 100 ng/mL TNFα (TNF group), or 100 ng/mL TNFα + 10^7 CFU/mL HY7302 (TNF + HY7302 group). (D) Western blot images of extracellular signal-regulated kinase (ERK), phospho-ERK (p-ERK), p38 mitogen-activated protein kinases (p38), phospho-p38 (p-p38), matrix metalloproteinase-9 (MMP-9), inteleukin-1 beta (IL-1β) and glyceraldehyde 3-phosphate dehydrogenase (GAPDH), and (E) phosphoprotein ratios or protein levels relative to vehicle-treated cells (CON group). For experimental groups, cells were treated with 100 ng/mL TNFα (T group), 100 ng/mL TNFα + 10^6 CFU/mL HY7302 (T + 10^6 group) or 100 ng/mL TNFα + 10^7 CFU/mL HY7302 (T + 10^7 group). $^{\#}p < 0.05$ and $^{\#\#\#}p < 0.001$ relative to CON group. $^{*}p < 0.05$, $^{**}p < 0.01$, and $^{***}p < 0.001$ relative to TNFα-only groups (TNF group in A-C and T group in D-E).

4. Discussion

DE, a multifactorial ocular surface disease, is characterized by tear film instability that correlates with symptoms and pathologies such as blurred vision, eye pain, and disruption of the ocular surface [47]. The etiology of DE is complex, and damage caused by increased ocular surface inflammation or apoptosis and corneal and conjunctival abnormalities contribute to DE pathogenesis [48]. Ocular surface desiccation is an important DE trigger factor. Prior studies have used mice, rats, and rabbits as animal models to investigate disease mechanisms of DE. In the BAC model, the ocular preservative BAC is administered to the ocular surface twice daily for 14 days. In the atropine model, DE is induced by administration of 1% atropine sulfate to the ocular surface three times daily for 5 days. Mouse models of Sjôgren syndrome are used to study spontaneous inflammatory DE. Desiccating stress, in which eyes are exposed to a constant low-humidity air flow for 4 h daily, can be used to induce DE. Aging animal models are also used to study DE [49]. In addition, the severity of DE in experimental animal studies is evaluated with DE tests, including the Schirmer tear test, corneal fluorescein staining, rose Bengal staining, and corneal sensitivity measured by esthesiometry.

In a prior study [36], we determined the effects of the *Limosilactobacillus fermentum* strain HY7302 in the DE mice model. We identified that oral administration of 1×10^9 CFU/kg/day HY7302 improves CFS score and TV. The effects of HY7302 on inflammatory signaling pathways in ocular tissue in BAC-treated cornea damaged mice has not been investigated. It is very important to assess the correlation of DE severity with potential changes in the gut microbiome mediated by HY7302 administration with the analysis of affected signaling pathways of eye tissue. Therefore, in the present study, we aimed to investigate the association between microbiome changes and severity of DE parameters correlated to inflammation, and to delineate the physiological and molecular mechanisms for HY3702 alleviation of DE.

In the present study, DE was induced with daily exposure to 0.1% BAC for 14 days. The efficacy of *L. fermentum* HY7302 at low and high doses (1×10^8 CFU/kg/day and 1×10^9 CFU/kg/day) was evaluated. As shown in our data, BAC-induced DE significantly decreased tear secretion, as measured by TV. Furthermore, DE increased CFS score and decreased TBUT. Treatment with HY7302 probiotics alleviated BAC-induced DE. Corneal epitheliums were dramatically detached in the BAC-induced DE group, while oral administration of HY7302 or omega3, used as a positive control, significantly alleviated detachment of the corneal epithelium. Together, these findings suggested that HY7302 probiotics significantly improved the phenotypes of BAC-induced DE.

Impaired tear production function in DE is related to environmental stressors of the ocular surface, which eventually cause chronic corneal epithelial damage and inflammation [50]. Inflammation contributes significantly to chronic ocular surface damage, and can impair tear film homeostasis, perpetuating a vicious cycle [51,52]. Destruction of the eye barrier by corneal dryness induces an inflammatory response to external pathogens and increases production of inflammatory cytokines, including TNF, IL-6, IL-8, and chemokines [25]. In the present study, p-JNK/JNK ratio and IL-1β protein level were significantly increased in the conjunctiva of the DE group relative to the CON group, as measured by Western blotting. However, these changes to phosphoprotein ratios and protein levels were alleviated in HY7302-treated groups relative to the DE group. Contrastingly, no differences in p-JNK/JNK ratio or IL-1β level were detected in the Omega3 positive control group

 doi:10.20944/preprints202402.1226.v1

relative to the DE group. The effect of HY7302 on MMP-9, which disrupts corneal epithelial barrier function, was also investigated, identifying that HY7302 treatment significantly decreased serum MMP-9 levels and the protein MMP-9 level in DE mice ocular tissue. Interestingly, according to our prior study [36], MMP-9 protein level of eye tissue significantly correlates with disease severity in BAC-induced DE. Consistently, in the present study, BAC-induced DE increased serum IL-20 levels, which was alleviated by HY7302 treatment but not significantly different. Therefore, our findings suggest that HY7302 probiotics inhibit the be systemic inflammatory response in tissue by regulating expression of MMP-9 and pro-inflammatory cytokines.

Importantly, DE is often accompanied by asymptomatic epithelial disease and abnormal inflammatory responses in the cornea and conjunctiva, which could be related to increased apoptosis in ocular tissues [53]. In Sjogren syndrome, a systemic inflammatory disease associated with DE, pathological cell death is an important disease mechanism [54]. Apoptosis is induced by activation of caspases, such as caspase-3, and is a normal homeostatic process that functions as a defense mechanism when cells are exposed to diverse noxious stimuli [55]. We identified that protein levels of apoptotic factors were affected in BAC-induced DE mice, with increased BAX and cleaved caspase 3 and decreased Bcl2. HY7302 treatment increased bcl-2 levels and decreased BAX and cleaved caspase 3 levels, suggesting decreased apoptosis. Interestingly, low-dose HY7302 treatment decreased BAX levels in DE mice more significantly than did high-dose HY7302 treatment. Thus, HY7302 intake could be more likely to have therapeutic effects in forms of DE associated with ocular epithelial inflammation and apoptosis.

Healthy aging is associated with changes to the gut-eye axis. Since the ocular surface environment and intestines are primary interfaces with the external environment, maintenance of inflammatory homeostasis in both organs is important for ocular function health related with tear secretion. The relationship between the gut microbiota and eye health has been underscored in recent findings. For example, studies of the gut–eye axis have demonstrated that the microbiota affects the pathogenesis of multiple eye diseases, including DE, age-related ocular disease, uveitis, and glaucoma [56,57]. Therefore, understanding the gut-ocular axis and role of the microbiome in eye disease is important for the development of new therapeutic approaches related to ingestion of functional probiotics to control the microbiome. Therefore, in the present study, we evaluated the effect of HY7302 intake on gut microbial communities by analyzing gut microbiota profiles. Alpha diversity, which represents changes to diversity in experimental groups, was assessed by determining the observed number of ASVs (Observed features). Also, beta diversity, which measures changes in diversity between groups, was determined by calculating the unweighted UniFrac distance to examine differences in the microbial community composition and structure. HY7302 modestly increased gut microbiota alpha diversity, but this change was not statistically significant. However, the beta diversity index significantly decreased between the CON and DE groups. Further, beta diversity index significantly increased in HY7302-treated groups relative to the DE group, suggesting improvement of gut microbiota diversity compared with the DE group. In addition, genus-level changes in the microbiomes of BAC-induced DE mice were partially reversed by HY7302 administration. The abundances of family Lachnospiraceae and family Muribaculaceae increased, while Oscillibacter decreased in HY7302-treated DE mice relative to untreated DE mice. Lachnospiraceae, Muribaculaceae, and Oscillibacter are cores of the gut microbiota community, and influence the overall health of the host. These populations affect immune system regulation and natural defenses against external infection [58].

In a recent study, gut microbiome analysis revealed compositional changes in Sjogren's syndrome, which is associated with decreased tear secretion and TBUT. Abundance of the genus Bifidobacterium is significantly decreased by Sjogren's syndrome, and overall beta diversity is decreased in Sjogren's syndrome which correlated with relative DE severity [59]. Likewise, in the present study, in species-level analyses, the relative abundances of *Clostridium leptum* and *Bacteroides caccae* were significantly decreased in the DE group relative to the CON group ($p = 0.002$ and $p = 0.010$, respectively). However, these populations were significantly increased in HY7302H-treated DE mice relative to untreated DE mice ($p = 0.009$ and $p = 0.036$, respectively). Recent studies have identified

 doi:10.20944/preprints202402.1226.v1

that Bacteroides spp. comprise a major fraction of the gut bacteriome and are important for maintenance of the gut microbial food web [60]. However, changes to normal dietary probiotics could induce hyperproliferation of Bacteroides spp., which could cause microbiome changes induced by other intestinal symbionts. Bacteroides caccae promotes mucus degradation, which reduces intestinal inflammation by decreasing bacterial interactions with epithelial cells of the large intestine. In addition, Colidextribacter abundance is significantly correlated with pro-inflammatory metabolites generated by the gut microbiome, suggesting that Colidextribacter could produce inflammatory metabolites [61]. We also identified that *Bifidobacterium pseudologum* abundance was significantly higher in the HY7302H-treated DE group than in the untreated DE group ($p = 0.033$). A recent study reported that *B. pseudolongum* is closely related to intestinal barrier enhance, regulating inflammation, oxidative stress, and tight junction protein levels in this context [62]. This suggests that in the present study, HY7302 treatment could have normalized the intestinal inflammatory response by increasing *B. pseudolongum* abundance. Together, microbiome analyses demonstrated that HY7302 could alleviate BAC-induced DE pathologies in ocular tissue by increasing the abundances of species associated with inflammation or other chronic ocular diseases. Future studies will aim to determine the physiological effects and metabolic profile of *L. fermentum* HY7302.

Recent studies have identified that inflammatory bowel disease (IBD), a common chronic intestinal inflammatory disease, is associated with DE. IBD has detrimental effects on extraintestinal systems such as the eye due to intestinal wall damage [36]. A significant relationship between IBD, ocular surface damage, and recurrent corneal erosion was also identified. Regarding on this, finally, in relation to the pathological microbiota mechanisms of DE and the immunomodulatory effects of HY7302 probiotics, we determined if HY7302 could improve tight junction function in the CMT-93 mouse colon epithelial cell line. Tight junction protein 1 (TJP-1), occludin-1 (OCLN-1), and claudin-4 (CLDN-4) maintain barrier function by regulating the permeability of intestinal epithelial cells. Further, pro-inflammatory cytokines such as IL-1β and IL-6 are released when tight junctions are damaged and permeability increases. The pro-inflammatory factor TNFα is an important regulator of the inflammatory process in this context, and affects MMP-9 production. We identified that treatment of CMT-93 cells with HY7302 increased mRNA levels of *TJP-1* and *OCLN-1* but did not affect *CLDN-4* mRNA levels. HY7302 treatment also increased *TJP-1* and *OCLN-1* mRNA levels in cells stimulated with TNFα. Also, HY7302 suppressed the inflammatory response to TNFa stimulation by decreasing *TNF*, *MMP-9*, and *IL-6* mRNA levels, p-ERK/ERK and p-p38/p38 ratios, and MMP-9 and IL-1 β protein levels in cells stimulated with TNFα. This suggests that HY7302 ingestion could alleviate the intestinal inflammatory response by increasing tight junction protein expression, which could indirectly decrease ocular tissue inflammation.

In conclusion, oral intake of *L. fermentum* HY7302 probiotics alleviated BAC-induced cornea damage. TV and TBUT increased, while CFS scores and corneal detachment injury index decreased, in DE mice treated with HY7302 relative to untreated DE mice. Moreover, HY7302 decreased DE-induced ocular inflammation and apoptosis and alleviated corneal epithelial detachment in this context. HY7302 treatment decreased inflammatory cytokine production and MMP-9 secretion in ocular tissue, which are important DE regulators. Further, HY732 increased microbiota beta-diversity and altered microbiome composition in the context of DE. Taken together, these findings suggest HY7302 could alleviate DE by regulating gut–eye axis communication via the inflammatory response. Therefore, HY7302 probiotics could potentially improve eye health by controlling intestinal health and immune regulation.

Author Contributions: Conceptualization, K.L. and J.Y.K.; methodology, K.L.; software, K.L., H.G.; validation, K.L.; formal analysis, K.L.; investigation, K.L.; data curation, K.L; writing—original draft preparation, K.L.; writing—review and editing, J.Y.K. and J.H.L.; visualization, K.L.; project administration, K.L., J.J.S., and J.H.L; All authors have read and agreed to the published version of the manuscript.

Funding: This research received no external funding.

Institutional Review Board Statement: The animal study protocol was approved by the Institutional Review Board of Institutional Animal Care and Use Committee (IACUC number P235002) in NDIC co., Ltd.

 doi:10.20944/preprints202402.1226.v1

Informed Consent Statement: Not applicable.

Data Availability Statement: The data presented in this study are available.

Funding: This study received no external funding.

Conflicts of Interest: The authors declare no conflict of interest. The authors declare no conflict of interest. We declare that the research was conducted in the absence of any commercial or financial relationships with hy.Ltd.company.

References

1. Rao, S.K.; Mohan, R.; Gokhale, N.; Matalia, H.; Mehta, P. Inflammation and dry eye disease—where are we? *International Journal of Ophthalmology* **2022**, *15*, 820.
2. Barabino, S. Is dry eye disease the same in young and old patients? A narrative review of the literature. *BMC ophthalmology* **2022**, *22*, 1-6.
3. Milner, M.S.; Beckman, K.A.; Luchs, J.I.; Allen, Q.B.; Awdeh, R.M.; Berdahl, J.; Boland, T.S.; Buznego, C.; Gira, J.P.; Goldberg, D.F. Dysfunctional tear syndrome: dry eye disease and associated tear film disorders–new strategies for diagnosis and treatment. *Current opinion in ophthalmology* **2017**, *28*, 3.
4. Javadi, M.-A.; Feizi, S. Dry eye syndrome. *Journal of ophthalmic & vision research* **2011**, *6*, 192.
5. Zhang, X.; Jeyalatha M, V.; Qu, Y.; He, X.; Ou, S.; Bu, J.; Jia, C.; Wang, J.; Wu, H.; Liu, Z. Dry eye management: targeting the ocular surface microenvironment. *International journal of molecular sciences* **2017**, *18*, 1398.
6. Hynnekleiv, L.; Magno, M.; Moschowits, E.; Tønseth, K.A.; Vehof, J.; Utheim, T.P. A comparison between hyaluronic acid and other single ingredient eye drops for dry eye, a review. *Acta ophthalmologica* **2024**, *102*, 25-37.
7. Yun, S.-w.; Son, Y.-H.; Lee, D.-Y.; Shin, Y.-J.; Han, M.J.; Kim, D.-H. Lactobacillus plantarum and Bifidobacterium bifidum alleviate dry eye in mice with exorbital lacrimal gland excision by modulating gut inflammation and microbiota. *Food & Function* **2021**, *12*, 2489-2497.
8. Goldstein, M.H.; Silva, F.Q.; Blender, N.; Tran, T.; Vantipalli, S. Ocular benzalkonium chloride exposure: Problems and solutions. *Eye* **2022**, *36*, 361-368.
9. Walsh, K.; Jones, L. The use of preservatives in dry eye drops. *Clinical Ophthalmology* **2019**, 1409-1425.
10. Brignole-Baudouin, F.; Desbenoit, N.; Hamm, G.; Liang, H.; Both, J.-P.; Brunelle, A.; Fournier, I.; Guerineau, V.; Legouffe, R.; Stauber, J. A new safety concern for glaucoma treatment demonstrated by mass spectrometry imaging of benzalkonium chloride distribution in the eye, an experimental study in rabbits. *PLoS One* **2012**, *7*, e50180.
11. Desbenoit, N.; Schmitz-Afonso, I.; Baudouin, C.; Laprévote, O.; Touboul, D.; Brignole-Baudouin, F.; Brunelle, A. Localisation and quantification of benzalkonium chloride in eye tissue by TOF-SIMS imaging and liquid chromatography mass spectrometry. *Analytical and bioanalytical chemistry* **2013**, *405*, 4039-4049.
12. Fortingo, N.; Melnyk, S.; Sutton, S.H.; Watsky, M.A.; Bollag, W.B. Innate immune system activation, inflammation and corneal wound healing. *International journal of molecular sciences* **2022**, *23*, 14933.
13. Mohamed, H.B.; Abd El-Hamid, B.N.; Fathalla, D.; Fouad, E.A. Current trends in pharmaceutical treatment of dry eye disease: A review. *European Journal of Pharmaceutical Sciences* **2022**, *175*, 106206.
14. Pflugfelder, S.C.; Bian, F.; de Paiva, C.S. Matrix metalloproteinase-9 in the pathophysiology and diagnosis of dry eye syndrome. *Metalloproteinases In Medicine* **2017**, 37-46.
15. Minaříková, M.; Fík, Z.; Štorm, J.; Helisová, K.; Ferrová, K.; Mahelková, G. Tear matrix metalloproteinase-9 levels may help to follow a ocular surface injury in lagophthalmic eyes. *Plos one* **2022**, *17*, e0274173.
16. Pflugfelder, S.C.; Farley, W.; Luo, L.; Chen, L.Z.; de Paiva, C.S.; Olmos, L.C.; Li, D.-Q.; Fini, M.E. Matrix metalloproteinase-9 knockout confers resistance to corneal epithelial barrier disruption in experimental dry eye. *The American journal of pathology* **2005**, *166*, 61-71.
17. Kook, K.Y.; Jin, R.; Li, L.; Yoon, H.J.; Yoon, K.C. Tear osmolarity and matrix metallopeptidase-9 in dry eye associated with Sjögren's syndrome. *Korean journal of ophthalmology: KJO* **2020**, *34*, 179.
18. Messmer, E.M.; von Lindenfels, V.; Garbe, A.; Kampik, A. Matrix metalloproteinase 9 testing in dry eye disease using a commercially available point-of-care immunoassay. *Ophthalmology* **2016**, *123*, 2300-2308.
19. Wang, H.-H.; Chen, W.-Y.; Huang, Y.-H.; Hsu, S.-M.; Tsao, Y.-P.; Hsu, Y.-H.; Chang, M.-S. Interleukin-20 is involved in dry eye disease and is a potential therapeutic target. *Journal of biomedical science* **2022**, *29*, 1-18.
20. Thursby, E.; Juge, N. Introduction to the human gut microbiota. *Biochemical journal* **2017**, *474*, 1823-1836.
21. Yoo, J.Y.; Groer, M.; Dutra, S.V.O.; Sarkar, A.; McSkimming, D.I. Gut microbiota and immune system interactions. *Microorganisms* **2020**, *8*, 1587.
22. Horrocks, V.; King, O.G.; Yip, A.Y.; Marques, I.M.; McDonald, J.A. Role of the gut microbiota in nutrient competition and protection against intestinal pathogen colonization. *Microbiology* **2023**, *169*, 001377.

23. Bu, Y.; Chan, Y.-K.; Wong, H.-L.; Poon, S.H.-L.; Lo, A.C.-Y.; Shih, K.C.; Tong, L. A review of the impact of alterations in gut microbiome on the immunopathogenesis of ocular diseases. *Journal of Clinical Medicine* **2021**, *10*, 4694.
24. Scuderi, G.; Troiani, E.; Minnella, A.M. Gut microbiome in retina health: the crucial role of the gut-retina axis. *Frontiers in Microbiology* **2022**, *12*, 726792.
25. Campagnoli, L.I.M.; Varesi, A.; Barbieri, A.; Marchesi, N.; Pascale, A. Targeting the gut–eye axis: An emerging strategy to face ocular diseases. *International Journal of Molecular Sciences* **2023**, *24*, 13338.
26. Natividad, J.M.; Verdu, E.F. Modulation of intestinal barrier by intestinal microbiota: pathological and therapeutic implications. *Pharmacological research* **2013**, *69*, 42-51.
27. Gensollen, T.; Iyer, S.S.; Kasper, D.L.; Blumberg, R.S. How colonization by microbiota in early life shapes the immune system. *Science* **2016**, *352*, 539-544.
28. Den Besten, G.; Van Eunen, K.; Groen, A.K.; Venema, K.; Reijngoud, D.-J.; Bakker, B.M. The role of short-chain fatty acids in the interplay between diet, gut microbiota, and host energy metabolism. *Journal of lipid research* **2013**, *54*, 2325-2340.
29. Bäumler, A.J.; Sperandio, V. Interactions between the microbiota and pathogenic bacteria in the gut. *Nature* **2016**, *535*, 85-93.
30. Rastogi, S.; Singh, A. Gut microbiome and human health: Exploring how the probiotic genus Lactobacillus modulate immune responses. *Frontiers in Pharmacology* **2022**, *13*, 1042189.
31. Ren, C.; Zhang, Q.; de Haan, B.J.; Zhang, H.; Faas, M.M.; de Vos, P. Identification of TLR2/TLR6 signalling lactic acid bacteria for supporting immune regulation. *Scientific reports* **2016**, *6*, 34561.
32. Cavalcante, R.G.; de Albuquerque, T.M.; de Luna Freire, M.O.; Ferreira, G.A.; Dos Santos, L.A.C.; Magnani, M.; Cruz, J.C.; Braga, V.A.; de Souza, E.L.; de Brito Alves, J.L. The probiotic Lactobacillus fermentum 296 attenuates cardiometabolic disorders in high fat diet-treated rats. *Nutrition, Metabolism and Cardiovascular Diseases* **2019**, *29*, 1408-1417.
33. de Luna Freire, M.O.; do Nascimento, L.C.P.; de Oliveira, K.Á.R.; de Oliveira, A.M.; dos Santos Lima, M.; Napoleao, T.H.; da Costa Silva, J.H.; Lagranha, C.J.; de Souza, E.L.; de Brito Alves, J.L. Limosilactobacillus fermentum strains with claimed probiotic properties exert anti-oxidant and anti-inflammatory properties and prevent cardiometabolic disorder in female rats fed a high-fat diet. *Probiotics and Antimicrobial Proteins* **2023**, *15*, 601-613.
34. Yoon, Y.; Kim, G.; Noh, M.-g.; Park, J.-h.; Jang, M.; Fang, S.; Park, H. Lactobacillus fermentum promotes adipose tissue oxidative phosphorylation to protect against diet-induced obesity. *Experimental & Molecular Medicine* **2020**, *52*, 1574-1586.
35. Mikelsaar, M.; Zilmer, M. Lactobacillus fermentum ME-3–an antimicrobial and antioxidative probiotic. *Microbial ecology in health and disease* **2009**, *21*, 1-27.
36. Lee, K.; Jeong, J.W.; Shim, J.J.; Hong, H.S.; Kim, J.Y.; Lee, J.L. Lactobacillus fermentum HY7302 Improves Dry Eye Symptoms in a Mouse Model of Benzalkonium Chloride-Induced Eye Dysfunction and Human Conjunctiva Epithelial Cells. *International Journal of Molecular Sciences* **2023**, *24*, 10378.
37. Bolyen, E.; Rideout, J.R.; Dillon, M.R.; Bokulich, N.A.; Abnet, C.C.; Al-Ghalith, G.A.; Alexander, H.; Alm, E.J.; Arumugam, M.; Asnicar, F. Reproducible, interactive, scalable and extensible microbiome data science using QIIME 2. *Nature biotechnology* **2019**, *37*, 852-857.
38. Callahan, B.J.; McMurdie, P.J.; Rosen, M.J.; Han, A.W.; Johnson, A.J.A.; Holmes, S.P. DADA2: High-resolution sample inference from Illumina amplicon data. *Nature methods* **2016**, *13*, 581-583.
39. Price, M.N.; Dehal, P.S.; Arkin, A.P. FastTree 2–approximately maximum-likelihood trees for large alignments. *PloS one* **2010**, *5*, e9490.
40. Katoh, K.; Misawa, K.; Kuma, K.i.; Miyata, T. MAFFT: a novel method for rapid multiple sequence alignment based on fast Fourier transform. *Nucleic acids research* **2002**, *30*, 3059-3066.
41. Quast, C.; Pruesse, E.; Yilmaz, P.; Gerken, J.; Schweer, T.; Yarza, P.; Peplies, J.; Glöckner, F.O. The SILVA ribosomal RNA gene database project: improved data processing and web-based tools. *Nucleic acids research* **2012**, *41*, D590-D596.
42. Bokulich, N.A.; Kaehler, B.D.; Rideout, J.R.; Dillon, M.; Bolyen, E.; Knight, R.; Huttley, G.A.; Gregory Caporaso, J. Optimizing taxonomic classification of marker-gene amplicon sequences with QIIME 2's q2-feature-classifier plugin. *Microbiome* **2018**, *6*, 1-17.
43. Lozupone, C.; Knight, R. UniFrac: a new phylogenetic method for comparing microbial communities. *Applied and environmental microbiology* **2005**, *71*, 8228-8235.
44. Lozupone, C.A.; Hamady, M.; Kelley, S.T.; Knight, R. Quantitative and qualitative β diversity measures lead to different insights into factors that structure microbial communities. *Applied and environmental microbiology* **2007**, *73*, 1576-1585.
45. Xiao, F.; Cui, H.; Zhong, X. Beneficial effect of daidzin in dry eye rat model through the suppression of inflammation and oxidative stress in the cornea. *Saudi Journal of Biological Sciences* **2018**, *25*, 832-837.

 doi:10.20944/preprints202402.1226.v1

46. Ling, J.; Chan, C.-L.; Ho, C.-Y.; Gao, X.; Tsang, S.-M.; Leung, P.-C.; Hu, J.-M.; Wong, C.-K. The Extracts of Dendrobium Alleviate Dry Eye Disease in Rat Model by Regulating Aquaporin Expression and MAPKs/NF-κB Signalling. *International Journal of Molecular Sciences* **2022**, *23*, 11195.
47. Uchino, M.; Schaumberg, D.A. Dry eye disease: impact on quality of life and vision. *Current ophthalmology reports* **2013**, *1*, 51-57.
48. Yu, L.; Yu, C.; Dong, H.; Mu, Y.; Zhang, R.; Zhang, Q.; Liang, W.; Li, W.; Wang, X.; Zhang, L. Recent developments about the pathogenesis of dry eye disease: Based on immune inflammatory mechanisms. *Frontiers in Pharmacology* **2021**, *12*, 732887.
49. Huang, W.; Tourmouzis, K.; Perry, H.; Honkanen, R.A.; Rigas, B. Animal models of dry eye disease: Useful, varied and evolving. *Experimental and Therapeutic Medicine* **2021**, *22*, 1-10.
50. Baudouin, C. A new approach for better comprehension of diseases of the ocular surface. *Journal francais d'ophtalmologie* **2007**, *30*, 239-246.
51. Han, Y.; Guo, S.; Li, Y.; Li, J.; Zhu, L.; Liu, Y.; Lv, Y.; Yu, D.; Zheng, L.; Huang, C. Berberine ameliorate inflammation and apoptosis via modulating PI3K/AKT/NFκB and MAPK pathway on dry eye. *Phytomedicine* **2023**, *121*, 155081.
52. Stern, M.E.; Beuerman, R.W.; Fox, R.I.; Gao, J.; Mircheff, A.K.; Pflugfelder, S.C. The pathology of dry eye: the interaction between the ocular surface and lacrimal glands. *Cornea* **1998**, *17*, 584-589.
53. Messmer, E.M. The pathophysiology, diagnosis, and treatment of dry eye disease. *Deutsches Ärzteblatt International* **2015**, *112*, 71.
54. Manganelli, P.; Fietta, P. Apoptosis and Sjögren syndrome. In Proceedings of the Seminars in arthritis and rheumatism, 2003; pp. 49-65.
55. Singh, V.; Khurana, A.; Navik, U.; Allawadhi, P.; Bharani, K.K.; Weiskirchen, R. Apoptosis and pharmacological therapies for targeting thereof for cancer therapeutics. *Sci* **2022**, *4*, 15.
56. Xue, W.; Li, J.J.; Zou, Y.; Zou, B.; Wei, L. Microbiota and ocular diseases. *Frontiers in cellular and infection microbiology* **2021**, 1047.
57. Zysset-Burri, D.C.; Morandi, S.; Herzog, E.L.; Berger, L.E.; Zinkernagel, M.S. The role of the gut microbiome in eye diseases. *Progress in retinal and eye research* **2023**, *92*, 101117.
58. Al Bander, Z.; Nitert, M.D.; Mousa, A.; Naderpoor, N. The gut microbiota and inflammation: an overview. *International journal of environmental research and public health* **2020**, *17*, 7618.
59. Moon, J.; Choi, S.H.; Yoon, C.H.; Kim, M.K. Gut dysbiosis is prevailing in Sjögren's syndrome and is related to dry eye severity. *PloS one* **2020**, *15*, e0229029.
60. Zafar, H.; Saier Jr, M.H. Gut Bacteroides species in health and disease. *Gut Microbes* **2021**, *13*, 1848158.
61. Kang, G.-U.; Park, S.; Jung, Y.; Jee, J.J.; Kim, M.-S.; Lee, S.; Lee, D.-W.; Shin, J.-H.; Koh, H. Exploration of Potential Gut Microbiota-Derived Biomarkers to Predict the Success of Fecal Microbiota Transplantation in Ulcerative Colitis: A Prospective Cohort in Korea. *Gut and liver* **2022**, *16*, 775.
62. Guo, W.; Mao, B.; Cui, S.; Tang, X.; Zhang, Q.; Zhao, J.; Zhang, H. Protective effects of a novel probiotic Bifidobacterium pseudolongum on the intestinal barrier of colitis mice via modulating the Pparγ/STAT3 pathway and intestinal microbiota. *Foods* **2022**, *11*, 1551.